NASA Technical Memorandum 88788

Microstructure-Property Relationships in Directionally Solidified Single Crystal Nickel-Base Superalloys

Rebecca A. MacKay and Michael V. Nathal
Lewis Research Center
Cleveland, Ohio

Prepared for
MiCon 1986: Optimization of Processing, Properties and Service Performance Through Microstructural Control
sponsored by ASTM Committee E-4
Philadelphia, Pennsylvania, May 15–16, 1986

NASA

MICROSTRUCTURE-PROPERTY RELATIONSHIPS IN DIRECTIONALLY SOLIDIFIED SINGLE CRYSTAL NICKEL-BASE SUPERALLOYS

Rebecca A. MacKay and Michael V. Nathal
National Aeronautics and Space Administration
Lewis Research Center
Cleveland, Ohio 44135

ABSTRACT

The purpose of this paper is to discuss some of the microstructural features which influence the creep properties of directionally solidified and single crystal nickel-base superalloys. γ' precipitate size and morphology, γ-γ' lattice mismatch, phase instability, alloy composition, and processing variations will be among the factors considered. Recent experimental results will be reviewed and related to the operative deformation mechanisms and to the corresponding mechanical properties. Special emphasis will be placed on the creep behavior of single crystal superalloys at high temperatures, where directional γ' coarsening is prominent, and at lower temperatures, where γ' coarsening rates are significantly reduced. It can be seen that very subtle changes in microstructural features can have profound effects on the subsequent properties of these materials.

E-3122

INTRODUCTION

A major advance in the investment casting of nickel-base superalloys occurred with the introduction of directional solidification (1). It was generally recognized that the fracture of polycrystalline materials at high temperatures was initiated at transverse grain boundaries. The columnar grain structure produced by directional solidification reduced the weakening influence of transverse grain boundaries and provided improved rupture ductility, creep lives, and thermal fatigue resistance over conventionally cast superalloys with an equiaxed grain structure (1,2). The development of single crystal superalloys was the next logical step after the production of

directionally solidified (DS) columnar grained material. The elimination of all of the grain boundaries offered the potential of operating at still higher temperatures.

However, it was found experimentally that [001]-oriented single crystals had only minor improvements in properties over the same alloy in columnar grained form (2-4). Thus, it became apparent that the development of alloys designed specifically for single crystal applications would be necessary for improved performance over DS materials (3-5). One major alloy modification was the removal of the grain boundary strengthening elements C, B, Zr, and Hf, which caused a significant increase in incipient melting temperature. This allowed higher heat treating temperatures that could more completely dissolve the coarse, primary γ' present in as-cast structures, so that the γ' phase could then be re-precipitated as a fine dispersion. Subsequent research has involved other compositional variations in order to obtain further improvements in metal temperature capability (4-6).

It is recognized that a number of mechanical and physical properties are important for turbine blade applications, and a discussion of all of these properties is beyond the scope of this paper. Thus, the present paper will focus specifically on the interrelation between microstructural features and creep properties in single crystal superalloys. This area has received a considerable amount of attention recently. It will be shown that some very subtle changes in microstructural features can have rather profound effects on the properties of these materials. Although many unanswered questions remain, a reasonably consistent picture of the operative creep mechanisms has been developed, which can provide some guidelines for alloy and process design. This review will be divided into two categories which represent different deformation mechanisms: creep around 1000 °C, where directional γ'

coarsening is prominent; and creep around 760 °C, where such coarsening is negligible.

SUPERALLOY MICROSTRUCTURE

Nickel-base superalloys derive much of their high temperature strength from a fine dispersion of the γ' precipitate. The typical as-heat treated microstructure of modern single crystal superalloys consists of approximately 60 vol % of the γ' precipitate dispersed in a matrix of γ. The γ' precipitate is usually in the form of cubes or spheres after heat treatment; examples of typical heat treated microstructures are shown in Fig. 1.

The initial γ' size and shape is determined by the details of the heat treatment as well as by the alloy composition. A typical heat treatment schedule consists of a solution treatment, a coating cycle, and a final age. The purpose of the solution treatment (typically 1300 °C/4 hr) is to dissolve the coarse as-cast γ' structures for subsequent re-precipitation as a fine dispersion. The homogenization of the dendritic segregation is perhaps of equal importance, in order to avoid heterogeneous γ' distributions. The size of the γ' particles is also strongly dependent on the cooling rate from the solution temperature (4,8). The heating cycle for application of a protective coating (typically 1000 °C/5 hr) can also cause some γ' coarsening. Changes in the parameters for this cycle have received renewed interest because this coating cycle has been demonstrated (9-11) to have a strong influence on properties. The final age (typically 870 °C/20 hr) may cause some additional coarsening. This age appears to have originated with the use of polycrystalline superalloys, and to the present authors, its effects on single crystals appears to be small.

The shape of small γ' particles is usually spherical, as a result of the minimization of surface energy. As the particles coarsen, their shape tends to change to a cuboidal morphology, which is due to the elastic

coherency strains between γ and γ', and to the elastic interaction between adjacent γ' particles (12,13). At larger sizes, the particles can become semi-coherent in some alloys and assume a more irregular shape (8,14). The semi-coherent γ' particles are characterized by regular arrays of misfit dislocations at the γ-γ' interface.

The following sections will consider the behavior of DS and single crystal materials during creep testing at elevated and intermediate temperature regimes. The initial as-heat treated structures will be shown to have considerable impact on creep properties. In these discussions, frequent reference is made to several specific alloys. Table I lists the compositions of these alloys.

CREEP AROUND 1000 °C

Raft Formation

Under an applied stress at elevated temperatures, the discrete γ' particles link up to form what are commonly called γ' rafts. Depending on the crystallographic orientation, the lattice and elastic modulus mismatch, and the sign of the applied stress, various rod or plate-like γ' morphologies can develop during creep deformation. In most modern superalloys with an [001] orientation, γ' plates form perpendicular to a tensile stress axis and parallel to a compressive stress axis at elevated temperatures (15). This type of directional coarsening has now been observed in a number of DS and single crystal alloys (7-11,15-20).

The microstructures in Fig. 2 illustrate the development of directional coarsening from a cuboidal to a plate-like morphology during creep. Similar raft development has been observed in both model (8,16) and commercial (7,15) alloys. It was found that directional coarsening begins rapidly during primary creep, as the γ' particles link up laterally without thickening. The raft thickness and interlamellar spacing remain constant throughout most

of the creep test, and this is an indication of the stability of the rafted structure once it is formed. These γ-γ' lamellar structures were more finely-spaced and more extensive laterally in comparison to the γ' stringers observed previously (21,22) in alloys with lower γ' volume fractions.

Pearson and co-workers (9,10) conducted the first studies on γ' directional coarsening in Alloy 143, a modern superalloy with a high γ' volume fraction. This alloy had exceptional creep properties around 1038 °C, not only because of its high refractory metal level, but also because of the γ' morphology which developed during subsequent creep testing. This was demonstrated by comparing the creep behavior of crystals given two different heat treatments: 1) a solution treatment and air cooling to room temperature; and 2) a solution treatment plus a simulated coating cycle of 1080 °C for 4 hr, and a final age of 870 °C for 16 hr. Subsequent testing of these two specimens at 1038 °C indicated that the solutioned only specimen had a creep life which was at least four times greater than that of the specimen given a simulated coating cycle plus age. The reason for this difference was attributed to the microstructural features which evolved during testing. The solutioned only material developed continuous, fine γ-γ' lamellae; whereas the specimen given the coating cycle had a much coarser and less well developed lamellar structure (10). This then led to the conclusion that a finely-spaced rafted structure has superior elevated temperature creep properties in comparison to the same alloy which does not undergo directional coarsening to the same extent.

The γ-γ' lamellae are believed to strengthen the material for creep, because the morphology of the γ' phase essentially eliminates γ' particle by-passing (9,10), which is the creep mechanism normally operative in conventional nickel-base superalloys at elevated temperatures and low stresses (23,24). By preventing the dominant creep mechanism from occurring under

these testing conditions, significant deformation can proceed only by the more sluggish process of shearing of the γ' phase. Evidence of γ' shearing has been observed in rafts during creep in CMSX-2 (11) and in NASAIR 100 (20). It has been further postulated (9,19,20) that this shearing mechanism is also inhibited by the densely-spaced networks of misfit dislocations which develop at the γ-γ' interfaces. Although shear through the γ-γ' interface is considered to be the rate limiting step in the deformation process, slip in the γ and γ' phases also appears to be important.

γ' Size Effects

MacKay and Ebert (8,16,19) further extended the work of Pearson by making quantitative measurements of the raft development in Alloy 143 during creep at various temperatures and stress levels. The development of rafting was examined for three different starting microstructures; Fig. 3 shows the three mean γ' particle sizes and the range of particle-matrix coherency produced by oil quenching, forced air quenching, and air quenching plus aging for 115 hr at 982 °C. The oil quenched crystals in Fig. 3(a) directionally coarsened at a rate which was at least a factor of ten faster than either the air quenched or aged single crystals in Figs. 3(b) and (c), respectively. The aligned and closely-spaced cuboidal particles in the oil quenched condition appeared to have hastened the development of the rafts, partly because the distance for diffusion was reduced. In addition, misfit dislocations at the γ-γ' interfaces can consume some of the elastic coherency strains present in the initial condition, thereby reducing the driving force for rafting. As a result, the lack of misfit dislocations in the oil quenched condition allowed the full driving force for directional coarsening to be present initially, thereby fostering a rapid rafting rate.

The three initial microstructures in Fig. 3 also had a significant effect on both the creep properties and the subsequent raft morphologies (8). As shown in Fig. 4 (a), the creep life could be increased by a factor of three, by reducing the initial particle size to 0.15 μm through an oil quench. It was found that the thickness of the rafts which formed was equal to the initial γ' size prior to testing. Thus, the oil quenched single crystals, which had the finest γ' size, also had the finest γ' raft thickness, and consequently, the largest number of γ-γ' interfaces per unit volume. Since it is believed that the interfaces are strong barriers to dislocation motion and γ' shearing, then a larger number of interfaces should reduce creep deformation and improve creep properties. Comparison of the fully developed lamellae in Fig. 5 with the corresponding creep curves in Fig. 4(a) shows that the properties improved as the raft thickness decreased and the number of γ-γ' interfaces increased.

However, Caron and Khan (11) have shown in single crystals of another nickel-base superalloy, CMSX-2, that a two-fold increase in creep life at 1050 °C was attained when the initial γ' size was increased from 0.30 to 0.45 μm, as illustrated in Fig. 4(b). The 0.45 μm particles were aligned along cube directions and were cuboidal in shape, whereas the 0.30 μm particles were more rounded in shape and randomly distributed. The rafts which developed from these two starting conditions are illustrated in Fig. 6. The two-fold improvement in creep life was attributed to the slightly more regular γ-γ' lamellae (Fig. 6(b)) which were observed after 20 hr of creep in the crystals having the initially larger γ' particles. It was postulated that dislocation by-passing would be more difficult in the rafted structure having the higher degree of perfection. However, one puzzling feature was that the microstructural differences between the two γ' morphologies in Fig. 6 did

not persist throughout the creep curve, as it was not possible to distinguish between the two rafted morphologies during the later stages of secondary creep (11).

As demonstrated in Fig. 4, the results described for the CMSX-2 alloy (11) are in direct contrast to those reported for Alloy 143 (8). Apparently in CMSX-2, the detriment of increasing the raft thickness was more than compensated for by the benefits of improving the perfection of the rafted structure. It should be noted that the increases in raft perfection in CMSX-2 were accomplished by an increase in γ' size. Secondly, only slight changes in raft perfection appeared to have a large effect on creep life in this alloy. Similar subtle improvements in perfection of the rafts in Alloy 143 can also be seen in Fig. 5, although this was accomplished by a decrease in initial γ' size. Further research is necessary in order to clarify the influences of γ' size and the relative importance of γ' plate refinement versus raft perfection. However, for both alloys, the optimum properties were achieved with an initial microstructure consisting of aligned and cuboidal γ'. The difference in magnitude of the lattice mismatch between CMSX-2 and Alloy 143 is a likely source for the different creep response observed as a function of initial γ' size. This will be discussed in more detail in the next section.

Lattice Mismatch

The sign and magnitude of the lattice mismatch between the γ matrix and the γ' precipitate is another factor which can influence the microstructure and creep resistance of DS and single crystal alloys. The unconstrained mismatch δ is given by Eq. (1), where a_γ and $a_{\gamma'}$ are the lattice parameters of the two phases:

$$\delta = \frac{2(a_{\gamma'} - a_\gamma)}{(a_{\gamma'} + a_\gamma)} \qquad (1)$$

The sign of δ determines the orientation of the rafted structure with respect to the applied stress (18,25,26). Although elastic modulus mismatch has also been shown to be important (18,27), it has been demonstrated that superalloys with negative and positive values of lattice mismatch form rafts perpendicular and parallel, respectively, to the applied tensile axis. Apparent exceptions to the above rule stem from using room temperature mismatch measurements to explain the orientation of the rafts. Figure 7 illustrates the effect of elevated temperature lattice mismatch on γ' raft orientation. It can be seen that the sign of the mismatch can change from positive to negative as temperature is increased (25,28).

Lattice mismatch can also influence the rate of directional coarsening by providing part of the driving force for that process. Nathal et al. (25) have shown that alloys with higher magnitudes of mismatch develop γ' rafts at a faster rate during creep. However, even alloys with lower levels of lattice mismatch (about -0.2 percent) had formed the rafted structure within the first 20 percent of their creep lives at low stress levels. Therefore, the rate of raft formation does not appear to be the major influence on creep properties under these testing conditions. Perhaps the major influence of lattice mismatch on high temperature creep behavior is through the strength of the γ-γ' interface. Higher magnitudes of δ would result in a finer misfit dislocation spacing at the interface, thus providing a stronger barrier to dislocation flow and reducing creep deformation. An additional barrier to γ' shearing may be provided by the segregation of refractory elements to the γ-γ' interface (10,29,30). Such segregation would be most prominent for alloys with high magnitudes of lattice mismatch and with high concentrations of refractory elements. Note that high magnitudes of lattice mismatch are considered to be desirable for creep resistance. This is in contrast to

previous beliefs (31-33) in which zero mismatch was considered optimal; however, in a recent re-examination of published data, little experimental support for this concept was established (25).

Another effect of mismatch is through the initial γ' particle morphology. Alloys with higher magnitudes of lattice mismatch undergo the transitions from spherical to cubic to irregular morphologies at smaller particle sizes during aging or upon quenching from the homogenization temperature. Thus, at a given γ' particle size, different alloys can have different γ' morphologies as a result of different magnitudes of mismatch; this is shown in Fig. 1 for alloys given a typical commercial heat treatment, producing a γ' size of about 0.25 μm. In addition, cubic γ' particles tend to be strongly aligned on [001] directions, whereas spherical particles are more randomly distributed. In turn, the initial γ' morphology influences the raft morphology which develops subsequently during creep. A structure consisting of aligned, cuboidal γ' particles promotes a relatively perfect rafted structure, whereas the more randomly distributed spherical particles produce more irregular lamellae.

This correlation between lattice mismatch, initial γ' morphology, and the subsequent raft morphology can explain some of the apparent discrepancies between the studies on CMSX-2 by Khan (11) and on Alloy 143 by MacKay (8). The mismatch of the Alloy 143 at 982 °C was measured to be -0.82 percent, by high temperature X-ray diffraction (25). Because of its high mismatch, this alloy exhibited aligned and cubic γ' particles even in the oil quenched material with γ' particles of 0.15 μm size. All coarser γ' structures examined by MacKay showed evidence of a semi-coherent interface, with the corresponding loss of the sharp cubic γ' shape. The mismatch of CMSX-2 at 1050 °C was determined to be -0.3 percent, according to TEM observations of

the dislocation spacings in CMSX-2 aged at 1050 °C and quenched to room temperature (18). With this lower mismatch value, CMSX-2 required a larger γ' size of 0.45 μm in order to assume a cuboidal γ' morphology. Thus, the different trends in raft perfection as a function of particle size can now be seen to have arisen from these two alloys being in different stages of γ' shape development as a result of different mismatch values.

If it were possible to quench a high mismatch alloy (i.e., Alloy 143) more rapidly to form γ' spheres, it would be informative to see if the random distribution of the initial spheres would develop into imperfect rafts which degrade the creep properties, in spite of the increase in the number of γ-γ' interfaces. For now, it can be concluded that both raft perfection and an increase in the number of interfaces may be influential. Additional studies are warranted in order to effectively describe the apparent differences between high and low mismatch alloys. It is also clear that different alloys have optimum creep properties at significantly different initial particle sizes. This is an important observation to remember when, for example, alloys are compared to see supposed compositional effects.

Alloying Effects

It is difficult to make generalizations about a particular element because of the sensitivity of properties to microstructural features and testing conditions, as has been discussed above. Temperature, applied stress, crystal orientation, and heat treatment must all be taken into account when alloy modifications are studied. Furthermore, an alloying element frequently effects several microstructural features simultaneously, and its roles can be changed by the presence or absence of other elements in the alloy. For example, the removal of grain boundary strengthening elements has allowed significant opportunities for alloy modification. With the reduction in carbon, those

refractory metals which were formerly tied up in carbides are now free to partition between the γ and γ' phases, thereby increasing the solid solution content in both the matrix and the precipitate. Undoubtably, these compositional changes have altered lattice mismatch, γ' volume fraction, diffusion rates, antiphase boundary and stacking fault energies, and numerous other properties.

One of the first elements examined specifically in single crystals was Co, because it was considered a strategic element with its availability uncertain in the early 1980's (34). An initial study (4) indicated that the removal of Co in single crystal MAR-M247 increased the creep life. In a subsequent study, Nathal and Ebert (35-36) investigated similar alloys in more detail and concluded that the major influence of Co was through the lattice mismatch. In alloys with 3 wt % Ta and 10 wt % W, a reduction in Co level increased lattice mismatch, thus providing increased creep strength for the reasons described previously. Cobalt did not appear to affect mismatch as strongly in alloys with Ta removed (35).

Removal of Co also resulted in precipitation of the W-rich precipitates α and μ in NASAIR 100 (35). The small quantities of α and μ did not appear to harm creep properties, since NASAIR 100 was stronger than the 5 percent Co alloy without μ. Again, this effect of Co is not general, since the MXON series of alloys, which have 6 wt % Ta and 8 wt % W, showed the reverse trend; i.e., an increased tendency for μ phase formation with an increase in Co content (37). Although Khan et al. suggested that this μ precipitation may degrade creep properties slightly (37), the influence of Co on mismatch in the MXON alloys should also be considered. In any case, both Nathal (7,20) and Khan (37) concluded that microporosity appeared to be a more significant defect than the small quantities of μ phase in the materials studied.

Although there is some incentive for minimizing the use of the strategic metal Ta, several modern alloys contain from 3 to 12 wt % Ta (5,6,37). Tantalum is considered to be beneficial for environmental resistance and castability (5). Tantalum also strongly improved creep properties in MAR-M247 type alloys by increasing lattice mismatch, γ' volume fraction, and solid solution hardening of γ' (35,36,38). However, its relative effectiveness compared to other refractory elements is unclear (7,35,36). In Alloy 143, Ta additions were not as effective as Mo in improving creep strength (39).

The effect of Mo content has been extensively examined in Alloy 143 single crystals. MacKay and Ebert (8) have shown that the creep life was decreased by a factor of three when the Mo content was increased from 13.9 to 14.6 wt %. The 13.9 wt % Mo alloy contained very few third phase (NiMo δ) precipitates, which indicated that this composition was close to saturation of the matrix; whereas significant quantities of the acicular δ phase precipitated during creep in the 14.6 wt % Mo-containing alloy. The rather dramatic decrease in life for a small change in Mo content was attributed to the δ needles, around which envelopes of γ' formed. This third phase caused discontinuities in the γ-γ' lamellae, such that mobile dislocations could then circumvent the γ-γ' interfaces, thereby reducing the effectiveness of the rafted microstructure.

Alloys with an undersaturated γ matrix also exhibited degraded properties with respect to a similar but saturated alloy. In a series of Alloy 143 compositions, the creep properties were reduced from 400 to 30 hr when the Mo content was decreased from 14.3 to 12.8 wt % (39). This result was associated with the 12.8 wt % alloy having an undersaturated matrix. Aigeltinger and Kersker (29) have suggested that a strong ordering tendency occurs between Ni and Mo, such that solute segregation to γ-γ' interfaces

and to mobile dislocations would increase the creep resistance of an alloy. These effects would be most prominent at or near saturation. Other refractory elements could produce similar effects on creep behavior as did Mo. Since both undersaturated (39) and supersaturated (8) alloys had reduced properties, it can be seen that a narrow compositional range exists within which the mechanical properties are optimized.

Rhenium appears to be becoming increasingly important as an alloying element in single crystal superalloys. Rhenium partitions strongly to and strengthens the γ phase, and additions of this element on the order of 2 to 6 wt % significantly reduce unstressed γ' coarsening rates, apparently because of its slow diffusion away from the γ-γ' interfaces (40). This is an indication of structural stability, which is probably reflected in improved creep properties as well.

Creep Anisotropy

The results described in the previous sections have mainly involved properties of [001]-oriented crystals. Although [001] is the preferred growth direction and thus is the easiest to produce, advanced processing techniques enable other orientations to be considered for application. As shown in Fig. 8(a), crystallographic orientation did not have a significant influence on the creep rupture lives of MAR-M200 (41) and MAR-M247 (42) single crystals at temperatures around 980 °C. This was the result of several slip systems becoming operative at elevated temperatures (41).

In contrast, some modern alloys such as Alloy 143 (10) and SC 7-14-6 (43) exhibited creep properties which were highly anisotropic at elevated temperatures. This behavior is illustrated for Alloy 143 in Fig. 8(b); Pearson and co-workers (10) attributed this anisotropy to the different γ' precipitate morphologies which developed during creep testing. For example, crystals with a [112]-orientation developed plates inclined 35° to the applied

stress axis, rod morphologies developed parallel to the applied stress in [110]-oriented crystals, and three interconnecting plates developed on cube planes in the [$\bar{1}$11]-oriented crystals.

However, the crystals given a simulated coating cycle in Ref. 10 presumably did not completely raft during creep, and yet these crystals still exhibited anisotropic creep properties. This suggests that other effects may be contributing to creep anisotropy besides γ' morphology. Shah (44) has shown that single phase Ni_3Al is also highly anisotropic, and clearly this effect is not due to precipitate shape. Refractory elements such as Ti, Nb, and Ta partition preferentially to γ' and may contribute to creep strengthening and anisotropy by changing the magnitude of APB energies on {111} and {001} planes (30). Thus, it seems possible that the compositions of the γ and γ' phases are also important in determining the anisotropy of superalloys.

CREEP AROUND 760 °C

At 760 °C, the diffusion rates are too slow for γ' rafting to occur to any significant extent. However, many of the same factors influence the creep properties at 760 °C, although in different ways from the behavior at temperatures around 1000 °C. The influence of γ' size, alloy composition, and crystal orientation will be discussed below.

γ' Size Effects

The effect of γ' precipitate size and shape on creep in the CMSX-2 alloy was investigated at 760 °C by Khan and co-workers (11,45). Two different heat treatments were employed: one promoted a microstructure with irregularly shaped and distributed γ' particles having mean sizes ranging from 0.25 to 0.35 μm; and the second provided aligned, cuboidal particles having a mean size of about 0.45 μm. The single crystals with the larger, cuboidal precipitates developed

a homogeneous deformation structure during primary creep and low steady-state creep rates. The microstructure with the irregularly-shaped particles experienced heterogeneous deformation during the primary creep stage, a large amount of primary creep strain, and a creep life which was about half that of the cuboidal material.

Khan (37,45) confirmed and extended this work in studies on other experimental alloys. For example, when the γ' size was reduced from 0.36 to 0.20 μm, the MXON alloy exhibited a heterogeneous deformation structure at the beginning of primary creep, in which the γ' particles were sheared by a/3<112> superlattice partial dislocations. This type of shearing mechanism is characterized by intrinsic/extrinsic stacking faults that extend over many precipitates, similar to that in Fig. 9(a). As seen in Fig. 10, this lead to a considerable extent of primary creep before the structure was uniformly strain hardened, which is necessary for the transition into steady-state creep. On the other hand, the material containing the larger γ' exhibited Orowan looping around the γ' particles by a/2<110> dislocations, such as that seen in Fig. 9(b). This deformation was much more homogeneous, as shown in Fig. 9(c). The homogeneous, dense networks of dislocations which formed at the γ-γ' interfaces promoted efficient strain hardening and limited the extent of primary creep. At the end of primary creep, shearing of individual γ' precipitates did occur by {111}<112> slip, although the stacking faults were confined to individual particles.

Thus, it can be seen that the specific deformation mechanism, either particle shearing or looping, influences the extent of primary creep, and in many alloys the amount of primary creep directly affects the minimum creep rates and rupture lives (11,37,42,45-47). The MXON alloy (45) is an exception to this trend, since a refinement in γ' size caused a change in the primary creep mechanism and in the amount of primary creep strain, and yet did not

affect the steady-state creep rate and rupture life. This may be related to the fact that both the fine and coarse particles were cuboidal in this alloy.

Alloying Effects

The influence of alloying additions has not been extensively studied during intermediate temperature creep. Khan and co-workers (37,45) investigated the effects of Co in the MXON alloy base during creep at 760 °C. When the Co content was raised from 5 to 7.5 wt %, the extent of primary creep became quite large, as illustrated in Fig. 11. Both the 5 and 7.5 Co MXON versions had cuboidal γ' of approximately the same size. Again, the extensive primary creep strain in the MXON-7.5 Co alloy was attributed to the heterogeneous nature of the primary creep deformation behavior, which was characterized by γ' shearing by {111}<112> slip over long distances. Leverant and co-workers (48) have suggested that elements such as Co, Mo, and Cr lower the stacking fault energy of the matrix, which facilitates the formation of <112>-type dislocations required for γ' shearing. Therefore, Khan suggests that the lowering of the SFE is primarily responsible for the large amount of primary creep strain observed when the Co content is increased (37).

However, an alternative explanation for the influence of Co on the primary creep behavior of MXON alloys appears to be equally plausible. Grose and Ansell (28) have shown, although in higher strain rate tests, that low misfit alloys have a tendency to deform by γ' particle shearing mechanisms, whereas high misfit alloys tend to exhibit particle by-passing mechanisms. Secondly, increasing the Co content in NASAIR 100 derivatives has been shown to decrease the magnitude of the lattice mismatch (25,35). Thus, it is possible that a decrease in the magnitude of mismatch accompanies the increase in Co level in the MXON alloy series, which in turn may be at least partially responsible for

the change in deformation mechanism from Orowan looping to γ' shearing. This explanation is also supported by the work of Dongliang et al. (47), who studied primary creep in DS alloys. They found that alloys with low mismatch accumulated high amounts of primary creep strain and showed evidence of deformation by particle shearing, whereas high mismatch alloys exhibited the particle by-passing mode of deformation and low extents of primary creep.

Creep Anisotropy

The creep rupture properties of MAR-M200 (41,49) and MAR-M247 (42,46) single crystals were found to have a strong dependence on orientation at temperatures around 760 °C. Primary creep occurred by slip on the {111}<112> slip systems (46,49). Second-stage creep began only after sufficient strain hardening occurred from the interaction of two or more intersecting {111}<112> slip systems (49). A summary plot of the influence of orientation on creep life is presented in Fig. 12 for MAR-M200 and MAR-M247 single crystals in this temperature regime. MacKay and Maier (46) found that the rupture lives were greatly influenced by the lattice rotations required to produce intersecting slip. Crystals which required large rotations to become oriented for intersecting slip exhibited the shortest creep lives, because these crystals experienced large primary creep strains and either 1) failed during primary creep, or 2) underwent high true stress levels at the onset of steady-state creep. Again, the relationship between primary creep strain, steady-state creep rate, and rupture life is evident.

At 760 °C, the CMSX-2 alloy (50) exhibited lower creep strengths as the orientations of the crystals deviated up to 15° from the [001]. However, this anisotropy was much less pronounced than that exhibited by MAR-M200 and MAR-M247. The reasons for this behavior are not clear at this time, although the present authors would like to suggest a few possibilities. First, the compositions of the γ' and γ phases may influence anisotropy, as was

discussed earlier. Secondly, it has been shown (47,51) that decreasing amounts of primary creep strain can result from lowering the applied stress levels. Since the amount of strain accumulated during primary creep is integrally related to creep life anisotropy (46), then it seems possible that higher applied stresses could enhance creep anisotropy in CMSX-2. Finally, Khan (11,37,45) has shown that γ' particle size and shape influence the extent of primary creep through the presence or absence of {111}<112> slip early in the primary creep stage, and this effect may also influence the degree of anisotropy.

CONCLUDING REMARKS

The improved strength of DS and single crystal superalloys is one of the major reasons for their successful introduction in gas turbine engines. Certainly, high creep strength must be balanced with other properties, such as thermomechanical fatigue, oxidation, and corrosion resistance, in order to achieve optimal performance. In addition, the complexity of an actual turbine blade cannot always be modeled in simple laboratory tests. Nevertheless, knowledge of the behavior of these materials during such controlled conditions can aid in the understanding of their response to complex stress and temperature cycles.

The elevated temperature creep behavior of modern superalloys indicates significant departures from past design philosophies. In earlier work, high mismatch was believed to enhance overaging processes where particle by-passing mechanisms became easier as the particles grew. This particle growth would have been particularly detrimental, since a continuous rafted structure could not be maintained in alloys with low γ' volume fractions, or in all grains of a polycrystalline material. In contrast, the directional coarsening in

modern high volume fraction alloys actually suppresses by-passing mechanisms. Consequently, it has been found that some of the strongest and most stable single crystal alloys are those with a large negative mismatch.

It is becoming apparent that each alloy has a narrow composition and microstructural range for optimum creep properties. Additionally, the optimum microstructure and composition for creep around 1000 °C may not be the same as that for creep at 760 °C. Although further work is necessary, it appears that a homogeneous distribution of cuboidal γ' particles is necessary for high creep strength. However, the optimum γ' size is a function of lattice mismatch and possibly other factors. In terms of alloy design, a refractory metal content close to the saturation limit of the γ and γ' phases appears to be optimum. However, an element such as Co, which at first glance would not be expected to have a significant effect, can be quite influential. It must be kept in mind, however, that differences in observed properties between alloys may be the result of non-optimized microstructures, rather than from any real compositional effects. In the future, control of the interrelationships between composition, crystal orientation, microstructure, and processing of single crystals can allow significant increases in turbine blade performance.

REFERENCES

1. VerSnyder, F.L. and Guard, R.W., Transactions of the American Society for Metals, Vol. 52, 1960, pp. 485-493.
2. Piearcey, B.J. and Terkelsen B.E., Transactions of the Metallurgical Society of AIME, Vol. 239, 1967, pp. 1143-1150.
3. Northwood, J.E., Metallurgia, Vol. 46, No. 7, July 1979, pp. 437-442.
4. Strangman, T.E., Hoppin III, G.S., Phipps, C.M., Harris, K., and Schwer, R.E., in Superalloys 1980, J.K. Tien, et al., Eds., American Society for Metals, Metals Park, OH, 1980, pp. 215-224.

5. Gell, M., Duhl, D.N., and Giamei, A.F., in Superalloys 1980, J.K. Tien, et al., Eds., American Society for Metals, Metals Park, OH, 1980 pp. 205-214.

6. Harris, K., Erickson, G.L., and Schwer, R.E., in Superalloys 1984, M. Gell, et al., Eds., AIME, New York, NY, 1984, pp. 221-230.

7. Nathal, M.V., and Ebert, L.J., in Superalloys 1984, M. Gell, et al., Eds., AIME, New York, NY, 1984 pp. 125-134.

8. MacKay, R.A. and Ebert, L.J., in Superalloys 1984, M. Gell, et al., Eds., AIME, New York, NY, 1984, pp. 135-144.

9. Pearson, D.D., Lemkey, F.D., and Kear, B.H., in Superalloys 1980, J.K. Tien, et al., Eds., ASM, Metals Park, OH, 1980, pp. 513-520.

10. Pearson, D.D., Kear, B.H., and Lemkey, F.D., in Creep and Fracture of Engineering Materials and Structures, B. Wilshire and D.R.J. Owen, Eds., Pineridge Press Ltd., Swansea, U.K., 1981, pp. 213-233.

11. Caron, P. and Khan, T., Materials Science and Engineering, Vol. 61, 1983, pp. 173-184.

12. Ardell, A.J., Nicholson, R.B., and Eshelby, J.D., Acta Metallurgica, Vol. 14, 1966, pp. 1295-1309.

13. Doi, M. and Miyazaki, T., in Superalloys 1984, M. Gell, et al., Eds., AIME, New York, NY, 1984, pp. 543-552.

14. Lasalmonie, A. and Strudel, J.L., Philosophical Magazine, Vol. 32, 1975, pp. 937-949.

15. Nathal, M.V. and Ebert, L.J., Scripta Metallurgica, Vol. 17, No. 9, Sept. 1983, pp. 1151-1154.

16. MacKay, R.A. and Ebert, L.J., Scripta Metallurgica, Vol. 17, No. 10, Oct. 1983, pp. 1217-1222.

17. Ohe, J. and Wakita, S., in Superalloys 1984, M. Gell, et al., Eds., AIME, New York, NY, 1984, pp. 93-102.

18. Fredholm, A. and Strudel, J.L., in Superalloys 1984, M. Gell, et al., Eds., AIME, New York, NY, 1984, pp. 211-220.

19. MacKay, R.A. and Ebert, L.J., Metallurgical Transactions A, Vol. 16A, No. 11, Nov. 1985, pp. 1969-1982.

20. Nathal, M.V. and Ebert, L.J., Metallurgical Transactions A, Vol. 16A, No. 3, Mar. 1985, pp. 427-440.

21. Sullivan, C.P., Webster, G.A., and Piearcey, B.J., Journal of the Institute of Metals, Vol. 96, 1968, pp. 274-281.

22. Tien, J.K. and Copley, S.M., Metallurgical Transactions, Vol. 2, No. 1, Jan. 1971, pp. 215-219.

23. Carry, C. and Strudel, J.L., Acta Metallurgica, Vol. 26, 1978, pp. 859-870.

24. Leverant, G.R., Kear, B.H., and Oblak, J.M., Metallurgical Transactions, Vol. 4, No. 1, Jan. 1973, pp. 355-362.

25. Nathal, M.V., MacKay, R.A., and Garlick, R.G., Materials Science and Engineering, Vol. 75, 1985, pp. 195-205.

26. Pineau, A., Acta Metallurgica, Vol. 24, 1976, pp. 559-564.

27. MacKay, R.A., "Morphological Changes of Gamma Prime Precipitates in Nickel-Base Superalloy Single Crystals," NASA TM-83698, 1984, p. 27.

28. Grose, D.A. and Ansell, G.S., Metallurgical Transactions A, Vol. 12A, No. 9, Sept. 1981, pp. 1631-1645.

29. Aigeltinger, E. and Kersker, M., Metals Forum, Vol. 4, No. 1-2, 1981, pp. 112-116.

30. Kear, B.H. and Pope, D.P., in Refractory Alloying Elements in Superalloys, J.K. Tien and S. Reichman, Eds., ASM, Metals Park, OH, 1984, pp. 135-151.

31. Decker, R.F., in Symposium on Steel Strengthening Mechanisms, Zurich, Climax Molybdenum Co., Greenwich, CT, 1969, pp. 147-170.

32. Davies, R.G. and Johnston, T.L., in Ordered Alloys: Structural Applications and Physical Metallurgy, B.H. Kear, et al., Eds., Claitors Publishing Division, Baton Rouge, 1970, pp. 447-474.

33. Stoloff, N.S., in The Superalloys, C.T. Sims and W.C. Hagel, Eds., Wiley, New York, 1972, pp. 79-111.

34. Tien, J.K., Howson, T.E., Chen, G.L., and Xie, X.S., Journal of Metals, Vol. 32, No. 10, Oct. 1980, pp. 12-20.

35. Nathal, M.V. and Ebert, L.J., Metallurgical Transactions A, Vol. 16A, No. 10, Oct. 1985, pp. 1849-1862.

36. Nathal, M.V. and Ebert, L.J., Metallurgical Transactions A, Vol. 16A, No. 10, Oct. 1985, pp. 1863-1870.

37. Khan, T., Caron, P., and Duret, C., in Superalloys 1984, M. Gell, et al., Eds., AIME, New York, 1984, pp. 145-156.

38. Nguyen, H.C., Pletka, B.J., and Heckel, R.W., in High-Temperature Alloys: Theory and Design, J.O. Stiegler, Ed., AIME, Warrendale, PA, 1984, pp. 381-400.

39. Giamei, A.F., Pearson, D.D., and Anton, D.L., in High-Temperature Ordered Intermetallic Alloys, C.C. Koch, et al., Eds., Materials Research Society, Pittsburgh, PA, 1985, pp. 293-308.

40. Giamei, A.F. and Anton, D.L., Metallurgical Transactions A, Vol. 16A, No. 11, Nov. 1985, pp. 1997-2005.

41. Kear, B.H. and Piearcey, B.J., Transactions of the Metallurgical Society of AIME, Vol. 239, 1967, pp. 1209-1215.

42. MacKay, R.A., Dreshfield, R.L., and Maier, R.D., in Superalloys 1980, J.K. Tien, et al., Eds., ASM, Metals Park, OH, 1980, pp. 385-394.

43. Dalal, R.P., Thomas, C.R., and Dardi, L.E., in Superalloys 1984, M. Gell, et al., Eds., AIME, New York, NY, 1984, pp. 185-197.

44. Shah, D.M., Scripta Metalurgica, Vol. 17, No. 8, Aug. 1983, pp. 997-1002.

45. Caron, P. and Khan, T., in Strength of Metals and Alloys, H.J. McQueen, et al., Eds., Pergamon Press, New York, NY, 1986.

46. MacKay, R.A. and Maier, R.D., Metallurgical Transactions A, Vol. 13A, No. 10, Oct. 1982, pp. 1747-1754.

47. Dongliang, L., Deliang, Y., and Chuanqi, S., Superalloys 1984, M. Gell, et al., Eds., AIME, New York, NY, 1984, pp. 199-210.

48. Leverant, G.R., Kear, B.H., and Oblak, J.M., Metallurgical Transactions, Vol. 2, No. 8, Aug. 1971, pp. 2305-2306.

49. Leverant, G.R. and Kear, B.H., Metallurgical Transactions, Vol. 1, No. 2, Feb. 1970, pp. 491-498.

50. Khan, T. Caron, P., Fournier, D., and Harris, K., Materiaux et Techniques, Vol. 73, Oct.-Nov. 1985, pp. 567-578.

51. Leverant, G.R. and Duhl, D.N., Metallurgical Transactions, Vol. 2, No. 3, Mar. 1971, pp. 907-908.

TABLE I. - NOMINAL COMPOSITIONS OF DS AND SINGLE CRYSTAL ALLOYS (WEIGHT PERCENT)

Alloy	Al	Ta	Ti	Cr	Mo	Co	W	Nb	Ni
MAR-M200[a]	5.0	---	2.0	9.0	----	10.0	12.0	1.0	bal.
MAR-M247[a]	5.5	3.0	1.2	8.5	0.7	10.0	10.0	---	↓
NASAIR 100	5.7	2.8	1.5	9.2	1.0	----	10.2	---	
Alloy 143	5.8	6.2	---	---	14.3	----	----	---	
SC 7-14-6	6.6	---	---	---	13.5	----	5.9	---	
CMSX-2[b]	5.6	5.8	0.9	8.0	0.6	4.6	7.9	---	
MXON	6.1	6.0	---	8.0	2.0	5.0	8.0	---	

[a]DS versions of these alloy usually contain C, B, Zr, and Hf.
MAR-M is a registered trademark of Martin Marietta Company.
[b]CMSX-2 is a registered trademark of Cannon-Muskegon Corporation.

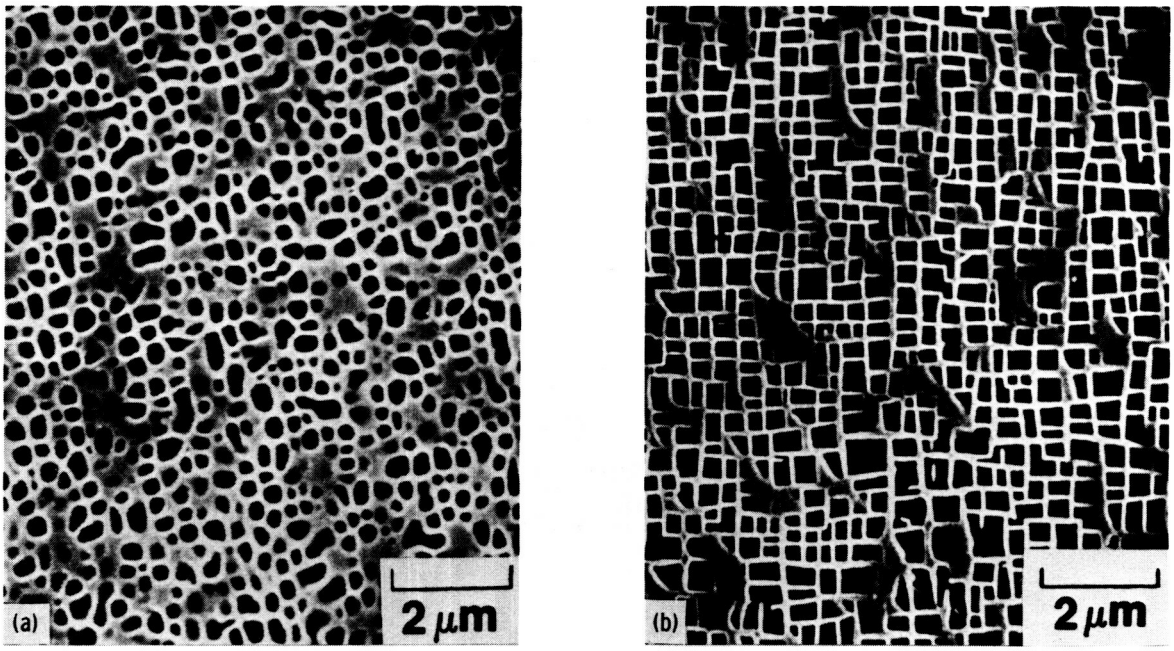

Figure 1. - Typical heat treated microstructures of superalloy single crystals showing (a) spherical and (b) cubic γ' particles. From reference 7.

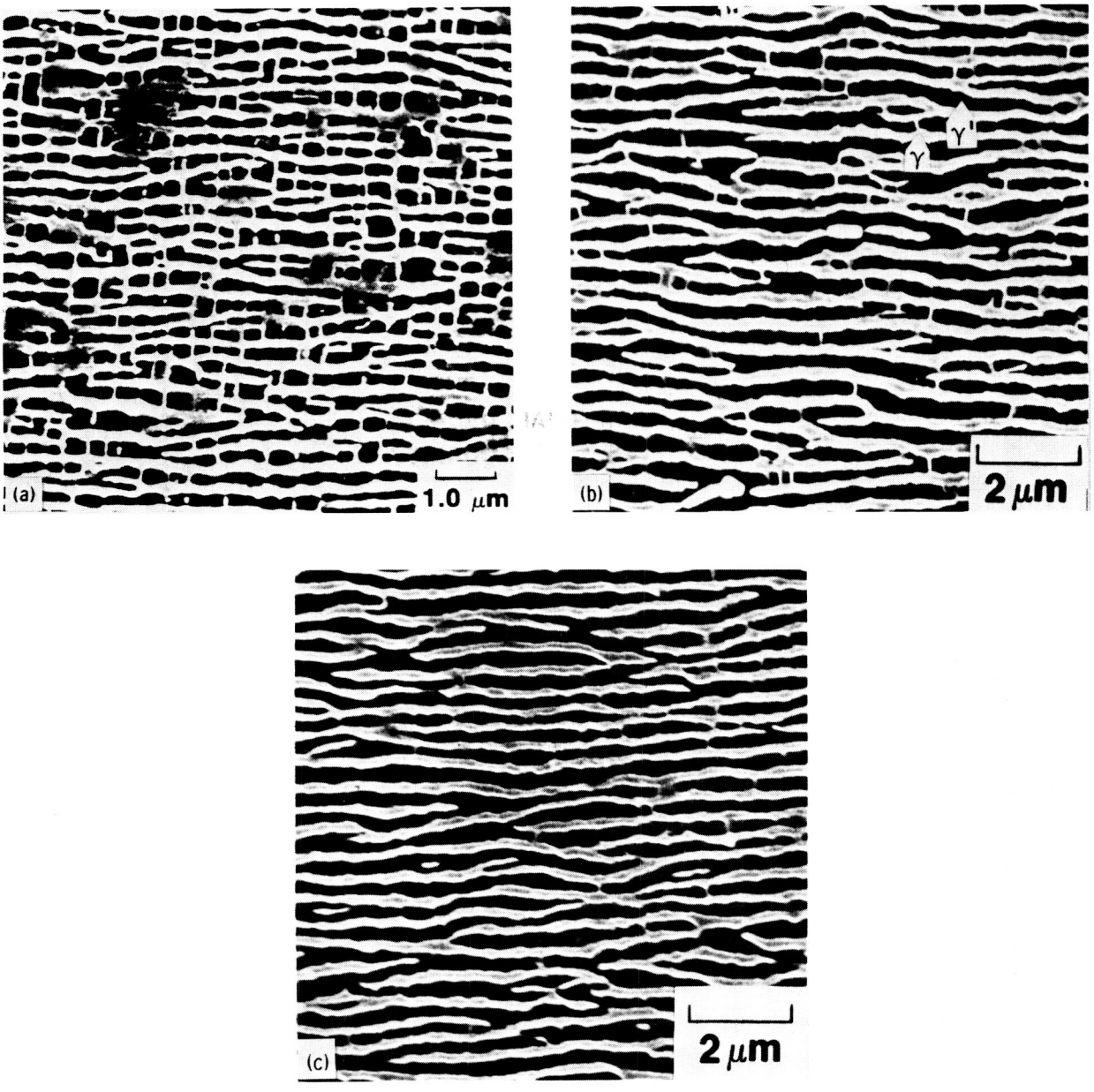

Figure 2. - Microstructures illustrating the development of directional γ' coarsening in NASAIR 100 during high temperature creep. The initial cubic γ' particles in Figure 1(b) merge laterally to form rafts perpendicular to the stress axis.

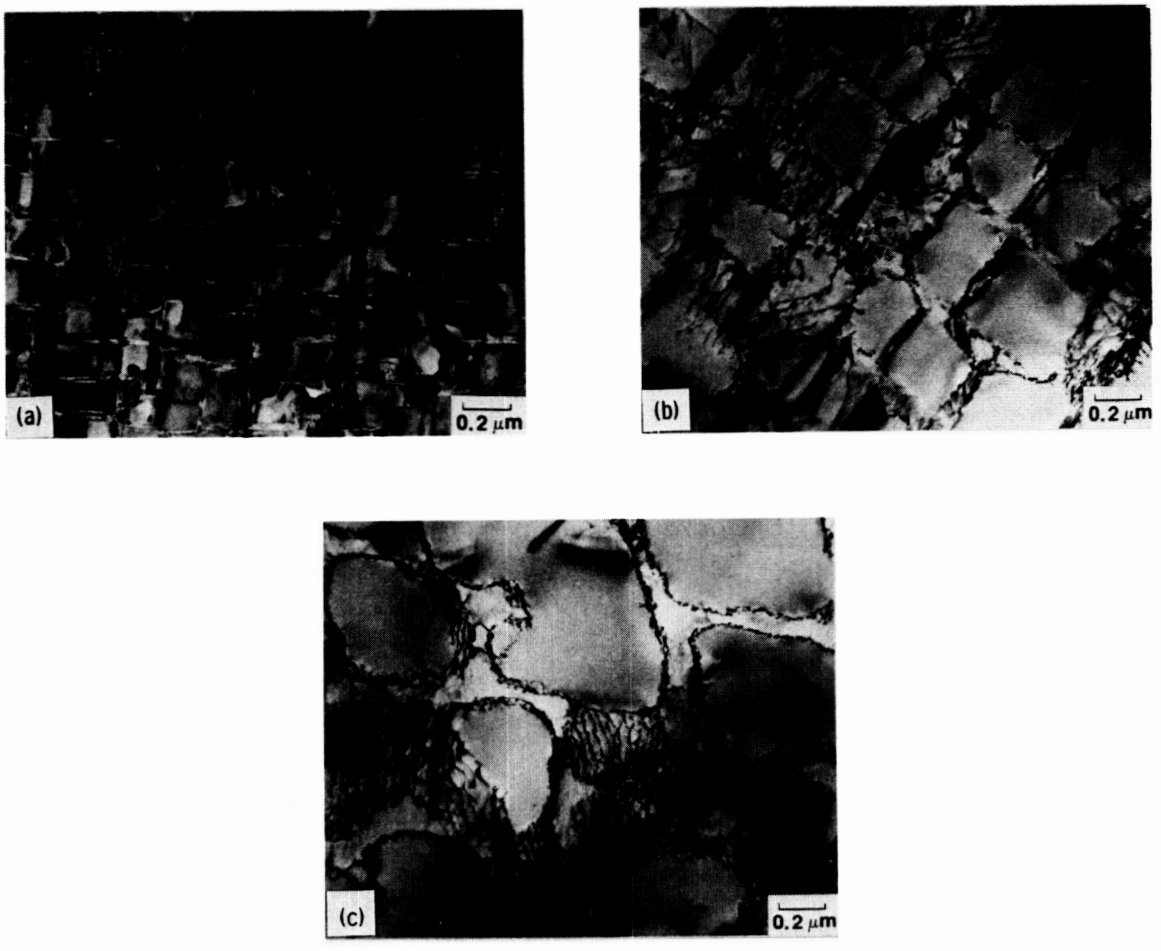

Figure 3. - The γ' precipitate and dislocation structure in Alloy 143 single crystals after solution treatment plus (a) oil quenching, γ' size=0.15 μm, (b) air quenching, γ' size=0.33 μm, and (c) air quenching plus aging at 982 ^{0}C/115 hours, γ' size=0.44 μm. From reference 8.

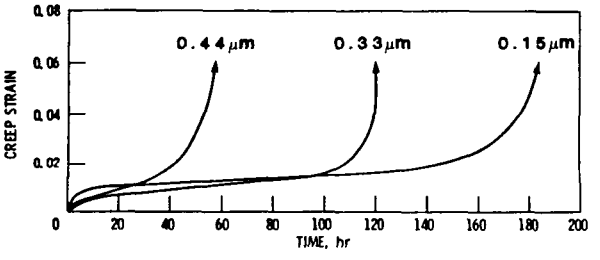

(a)

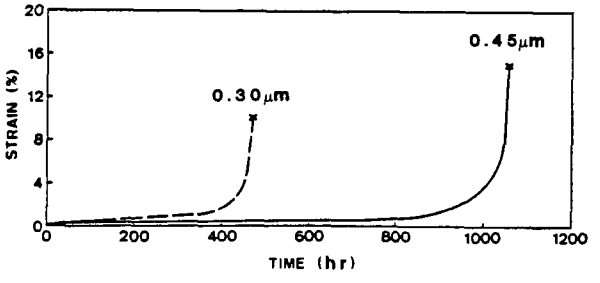

(b)

Figure 4. - Influence of initial γ' size on the creep curves of (a) Alloy 143 at 982 ^{0}C/234 MPa (ref. 8) and (b) CMSX-2 at 1050 ^{0}C/120 MPa (ref. 11).

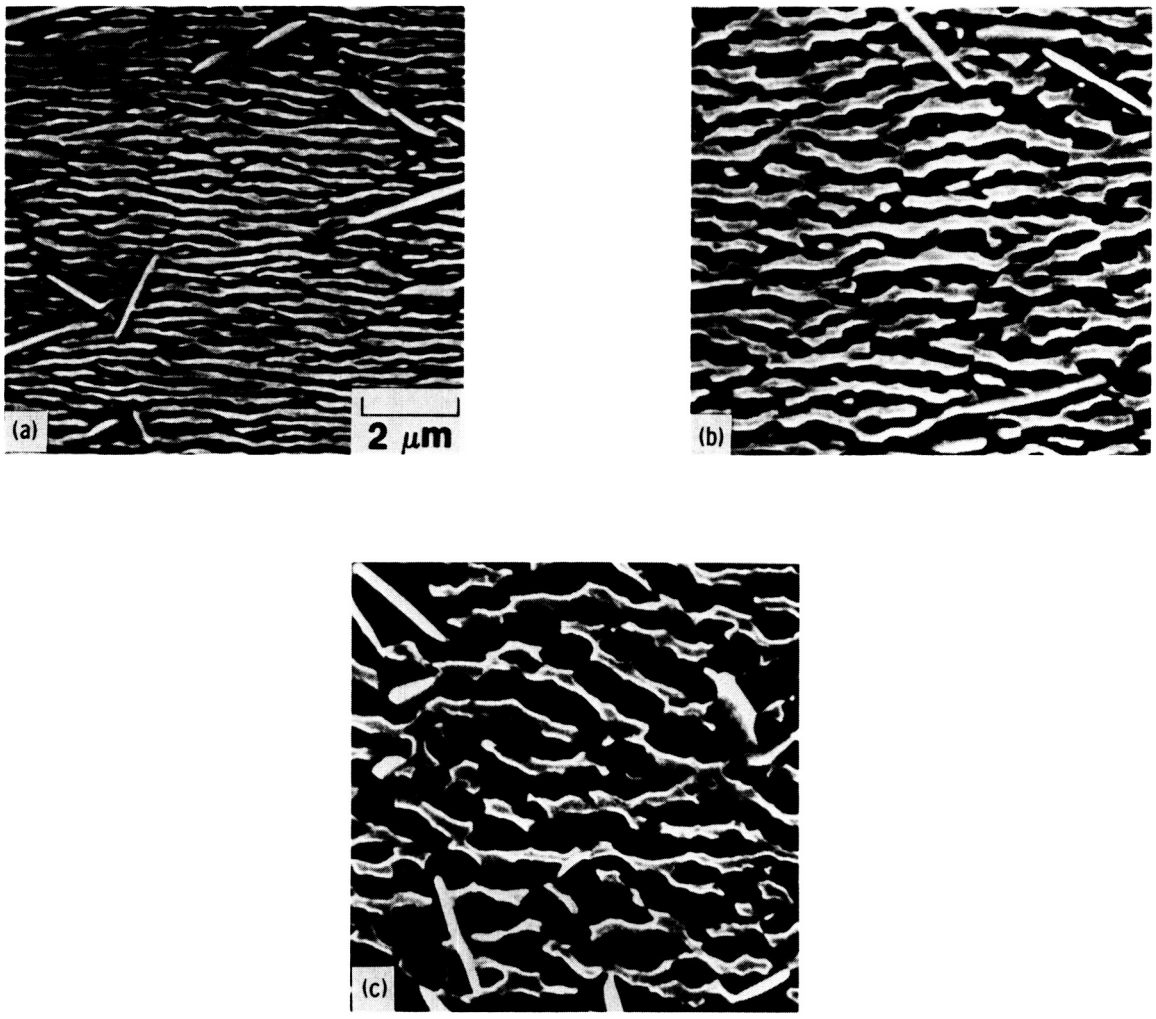

Figure 5. - Lamellar structures which developed in Alloy 143 after 50 hours of creep testing at 982 ^{o}C/234 MPa in the (a) oil quenched, (b) air quenched, and (c) aged conditions. From reference 8.

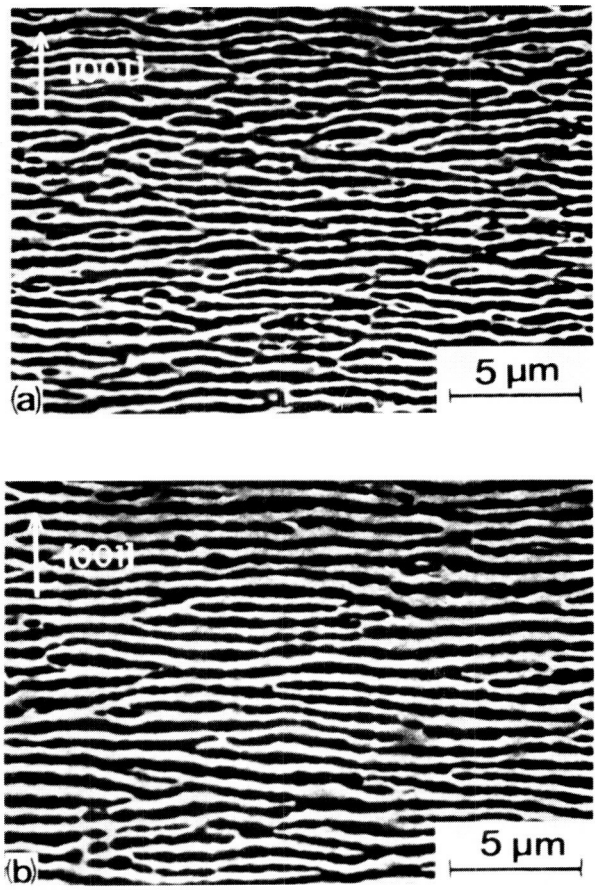

Figure 6. - Lamellar structures which developed in CMSX-2 single crystals after 20 hours of creep testing at 1050 ^{0}C/ 120 MPa having initial γ' sizes of (a) 0.30 μm and (b) 0.45 μm. From reference 11.

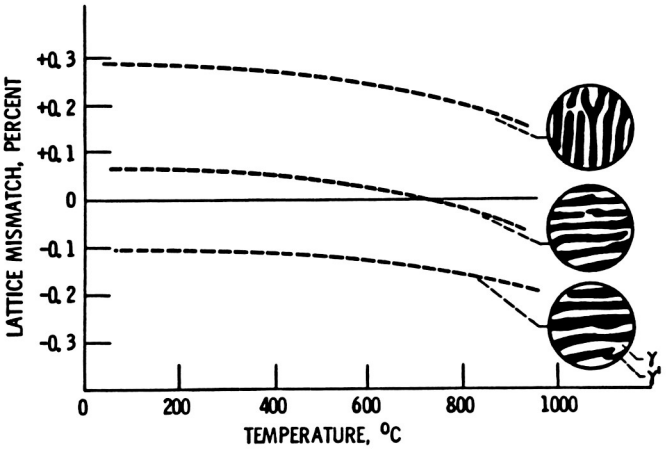

Figure 7. - Influence of elevated temperature lattice mismatch on γ' raft orientation.

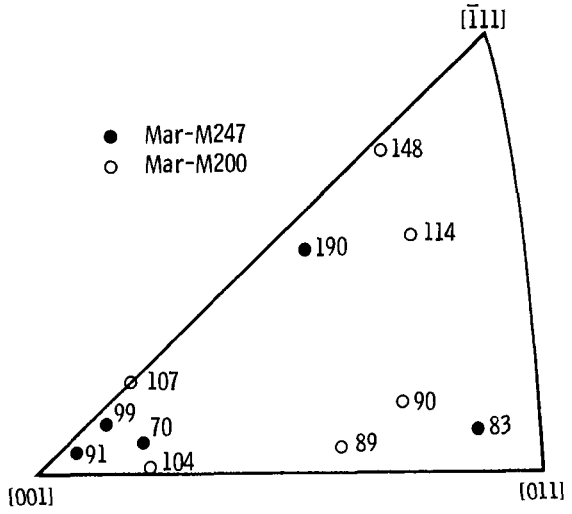

(a)

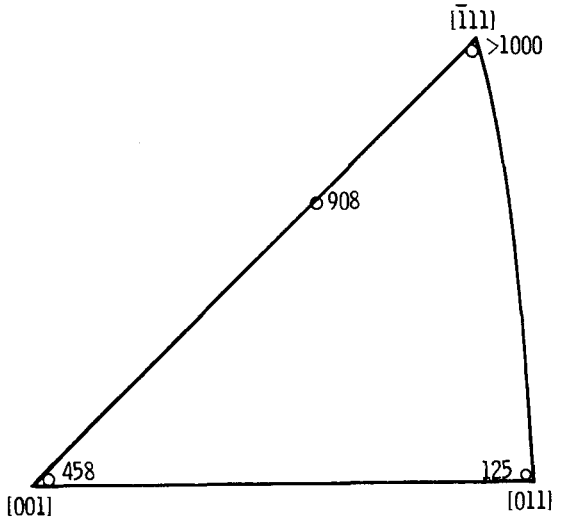

(b)

Figure 8. - High temperature creep lives of single crystals of various orientations. (a) Mar-M247 (ref. 42) and Mar-M200 (ref. 4) at 982 ^{0}C/207 MPa and (b) Alloy 143 (ref. 10) at 1038 ^{0}C/207 MPa.

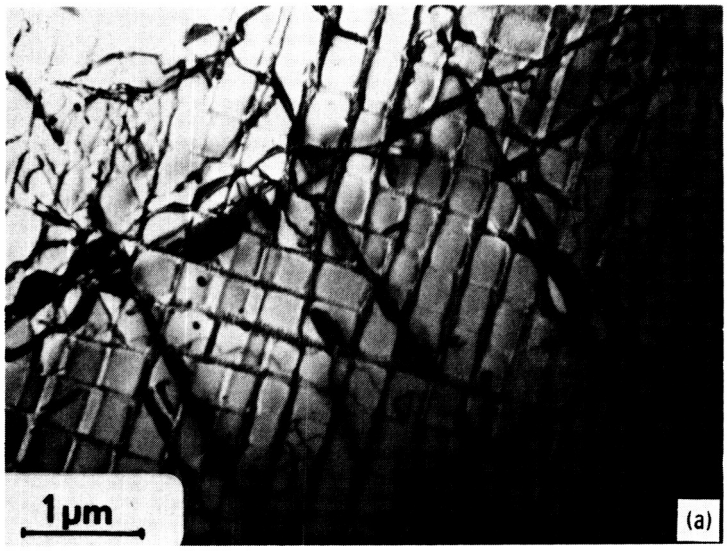

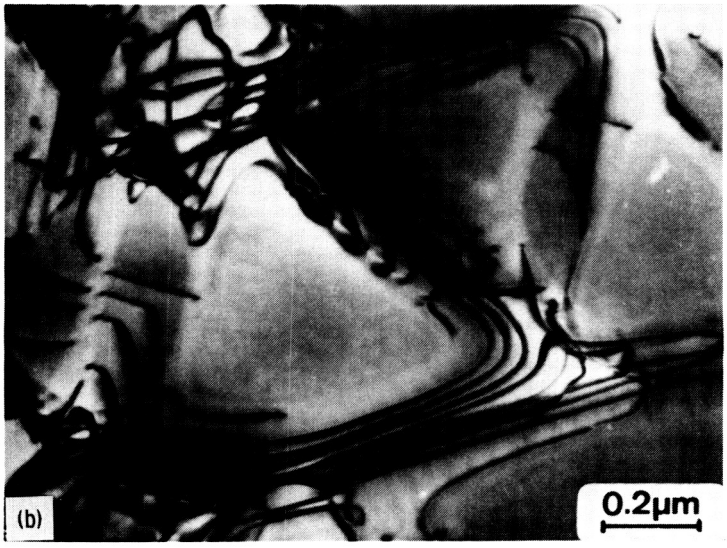

Figure 9. - Typical deformation structures observed during primary creep at 760 ^{0}C. (a) γ' particle shearing by intrinsic/extrinsic stacking faults. (b) Orowan looping around γ' particles. (c) Homogeneous dislocation distribution associated with the looping process. From references 11 and 37.

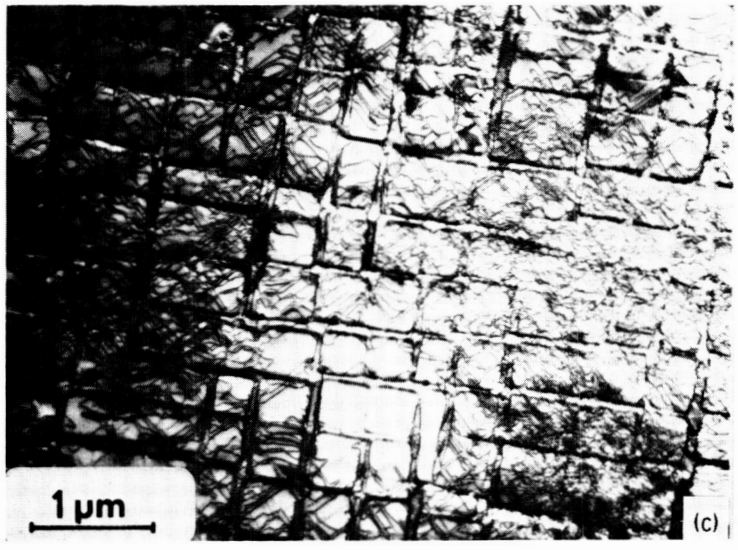

Figure 9. - Concluded.

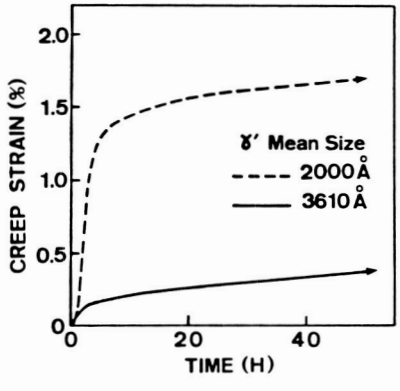

Figure 10. - Influence of γ' particle size on primary creep of MXON at 760 ^{0}C/750 MPa. From reference 37.

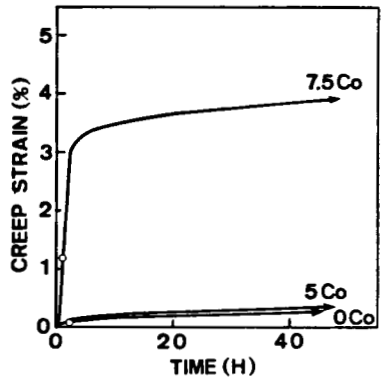

Figure 11. - Influence of Co level on primary creep behavior of MXON single crystals at 760 °C/ 750 MPa. From reference 37.

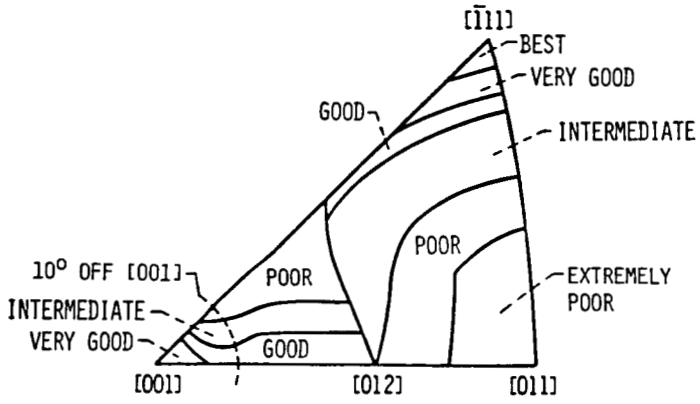

Figure 12. - Suggested regimes of creep rupture lives for Mar-M247 and Mar-M200 single crystals at about 760 °C. From reference 46.

1. Report No.	2. Government Accession No.	3. Recipient's Catalog No.
NASA TM-88788		

4. Title and Subtitle	5. Report Date
Microstructure-Property Relationships in Directionally Solidified Single Crystal Nickel-Base Superalloys	6. Performing Organization Code: 505-63-01

7. Author(s)	8. Performing Organization Report No.
Rebecca A. MacKay and Michael V. Nathal	E-3122
	10. Work Unit No.

9. Performing Organization Name and Address	11. Contract or Grant No.
National Aeronautics and Space Administration Lewis Research Center Cleveland, Ohio 44135	13. Type of Report and Period Covered: Technical Memorandum

12. Sponsoring Agency Name and Address	14. Sponsoring Agency Code
National Aeronautics and Space Administration Washington, D.C. 20546	

15. Supplementary Notes

Prepared for MiCon 1986: Optimization of Processing, Properties and Service Performance Through Microstructural Control, sponsored by ASTM Committee E-4, Philadelphia, Pennsylvania, May 15-16, 1986.

16. Abstract

The purpose of this paper is to discuss some of the microstructural features which influence the creep properties of directionally solidified and single crystal nickel-base superalloys. γ' precipitate size and morphology, γ-γ' lattice mismatch, phase instability, alloy composition, and processing variations will be among the factors considered. Recent experimental results will be reviewed and related to the operative deformation mechanisms and to the corresponding mechanical properties. Special emphasis will be placed on the creep behavior of single crystal superalloys at high temperatures, where directional γ' coarsening is prominent, and at lower temperatures, where γ' coarsening rates are significantly reduced. It can be seen that very subtle changes in microstructural features can have profound effects on the subsequent properties of these materials.

17. Key Words (Suggested by Author(s))	18. Distribution Statement
Nickel-base superalloys; Creep; Gamma prime; Mechanical properties; Single crystals; Precipitation; Directionally solidified alloys	Unclassified - unlimited STAR Category 26

19. Security Classif. (of this report)	20. Security Classif. (of this page)	21. No. of pages	22. Price*
Unclassified	Unclassified		

*For sale by the National Technical Information Service, Springfield, Virginia 22161